Strong Species Dependence of High Order Photoelectron Production in Alkali Metal Atoms

M. B. Gaarde,[1] K. J. Schafer,[2] K. C. Kulander,[3] B. Sheehy,[4] Dalwoo Kim,[4,5] and L. F. DiMauro[4]

[1]*Department of Physics, Lund Institute of Technology, P.O. Box 118, S-22100 Lund, Sweden*
[2]*Department of Physics and Astronomy, Louisiana State University, Baton Rouge, Louisiana 70803-4001*
[3]*TAMP, Lawrence Livermore National Laboratory, Livermore, California 94551*
[4]*Brookhaven National Laboratory, Upton, New York 11973*
[5]*Department of Physics, RIST, Pohang, Korea*
(Received 30 September 1999)

We present a theoretical and experimental study of the production of very high order photoelectrons from alkali metal atoms interacting with intense, midinfrared radiation. The strength of this process shows an unexpectedly strong species dependence. We find that this dependence can be explained via the difference in the cross section for electron-ion scattering from the different atoms. This allows us to directly relate the high energy portion of the photoelectron spectrum to specific features of the electron-ion potential.

The past decade has seen advances in both the fundamental understanding and the application of strong field multiphoton physics, in particular, intense field photoionization [1]. This has been facilitated by the increased resolution with which above threshold ionization (ATI) photoelectron spectra can be measured using high repetition rate, short pulsed lasers [2]. Recent studies have emphasized the effects caused by the interaction of an electron with its own ion core after it has been initially ionized and accelerated in the intense field [2–5]. The production of high energy photoelectrons, corresponding to the absorption of hundreds of photons above the ionization threshold [4,5], is among the most dramatic results of this interaction. Rather than steadily decreasing as one would expect if all the energy were gained at the time of ionization, the photoelectron spectrum exhibits a change of slope and a plateau before cutting off at a characteristic energy. Studies on rare gas atoms using intense visible/near-infrared radiation have found that the strength of this plateau relative to the total ionization yield depends upon both the atomic species and the intensity of the driving field [4,5].

In this Letter we use intense midinfrared (MIR) radiation to study the equivalent multiphoton process in alkali metal atoms. These are true one (valence) electron systems and, as such, enable us to exclude correlation effects in the formation of the high energy plateau. Unexpectedly, we find that the species dependence of the onset and strength of the plateau in these atoms is much more pronounced than in the rare gases. For example, potassium is found to exhibit a very strong plateau, whereas sodium shows almost no high order photoelectron production. We can explain this strong atomic species dependence in terms of a small change in the ionic potential, which has a large effect on the elastic scattering of the electron from the ion core. This allows us to directly relate the strength of the high energy portion of the photoelectron spectrum to specific features of the electron-ion potential.

The intensity and species dependence of the production of high order photoelectrons was initially observed in the angular distributions of the high energy electrons produced in xenon and krypton [6]. Fully nonperturbative, time-dependent calculations using the single active electron (SAE) approximation [2,5,6] reproduce the intensity scaling of both the angular distributions and the strength of the plateau. In the high intensity, long wavelength limit a simple description of high energy photoelectron production can be given in terms of the creation of a wave packet each half-cycle of the laser field via tunneling [6]. Classically, the cycle averaged kinetic energies (drift energies) of this wave packet are between 0 and $2U_p$, where U_p is the intensity and wavelength-dependent ponderomotive potential; see Ref. [7]. A significant portion of the wave packet is driven back into the vicinity of the ion core by the oscillating laser field. The energy of the wave packet at the time of return to the core is between 0 and $3U_p$. After scattering from the ion core it can be reaccelerated by the laser field, gaining additional drift energy. Again the energies can be estimated classically, and can be as high as $10U_p$ [5,8–10]. The electronic trajectories which have the highest kinetic energy at the time of scattering give rise to the largest drift energies after backward scattering from the ion core [8–10].

In this Letter we present theoretical and experimental photoelectron spectra for potassium, rubidium, and sodium interacting with strong 1.9 ps MIR pulses, covering a range of intensities up to saturation. The development of long wavelength lasers, capable of producing intense radiation at wavelengths between 3 and 4 μm [11], enables the observation of multiphoton processes in a broad class of systems with low ionization potentials (I_p). The alkali metals, with binding energies of 4–5 eV, belong to this group. The only previously studied one electron system with respect to the generation of a plateau is hydrogen, which was found to exhibit only a small production of high order photoelectrons [12]. The strong species dependence that we find in

the alkali metals emphasizes the importance of the atomic structure for the scattering efficiency even when the rescattering takes place in the strong field regime.

The calculation of the ATI spectrum is carried out by direct numerical integration of the time-dependent Schrödinger equation for the full laser-atom interaction within the SAE approximation [13]. To help interpret these results we also calculate the differential cross section for electron-ion elastic scattering. To describe the electron-ion interaction, we use the semiempirical pseudopotentials given in [14], to which we refer the reader for additional details. These potentials have three parts, a short range term V_{sr}, a polarization term V_{pol}, and a $-1/r$ potential at long range. Both the V_{sr} and the V_{pol} terms are strongly dependent on the atomic structure. The short range term represents the shielding of the nuclear charge by the core electrons, as well as the orthogonality constraints imposed by the exclusion principle. The polarization of the ion charge cloud is accounted for through dipole and quadrupole potentials. To ensure that the pseudopotential energies match the experimental energies as closely as possible, we use short range and polarization terms that are dependent on the angular momentum channel. The potential is thus nonlocal. However, the range over which it is nonlocal is restricted to distances where V_{sr} and V_{pol} are nonzero. It is also possible to construct local, spherically symmetric pseudopotentials which treat only the lowest angular momentum channel accurately. We will comment on the results obtained with these potentials below.

The choice of electromagnetic gauge has a large influence on the numerical effort involved in calculating the ATI spectrum. Close to the ion core, the $\mathbf{E} \cdot \mathbf{r}$ interaction (length gauge) is preferred, while at large distances use of the $\mathbf{A} \cdot \mathbf{p}$ interaction (velocity gauge) minimizes the number of angular momentum channels needed [15]. The two gauges are not equivalent when the pseudopotential is nonlocal. We have developed a mixed-gauge approach which uses the length gauge near the ion core and the velocity gauge at large distances. We switch gauges in a *transition zone* which is outside the region where the pseudopotential is nonlocal. This method allows us to use nonlocal pseudopotentials, which give a superior description of the atomic potentials as compared to local pseudopotentials, while minimizing the numerical effort.

We use a trapezoidal laser pulse with a one cycle turn-on, a five cycle plateau, and a one cycle turn-off to simulate a quasiconstant laser intensity. The laser wavelength is 3.2 μm, corresponding to a photon energy of 0.39 eV. Ionization of, for instance, K, with an I_p of 4.3 eV, thus requires a minimum of 11 photons.

Tunable MIR light is generated by difference frequency mixing the synchronized outputs of amplified Ti:sapphire and Nd:YLF mode-locked lasers. The MIR system produces linearly polarized 1.9 ps, 100 μJ pulses at a 1 kHz repetition rate over the wavelength range from $3-4$ μm

[11]. A collimated alkali metal atomic beam is produced by an effusive oven, the temperature of which controls the atomic density. The interaction chamber consists of a parabolic mirror time-of-flight electron energy spectrometer with a 2π collection angle. The spectrometer linearity has been calibrated by studying the ATI spectrum of xenon using 1.9 ps, 0.8 μm light. The MIR light is focused by an $f/4$ silicon lens at the focus of the electrostatic parabolic mirror. It is focused to a 40 ± 5 μm waist which gives a maximum intensity of 3 TW/cm^2.

Figure 1 shows total (angle integrated) ATI spectra in K and Na using 3.2 μm radiation. The spectra shown in Fig. 1(a) are calculated at an intensity of 1 TW/cm^2 and are representative of calculations over a range of laser intensities. The experimental spectra plotted in Fig. 1(b) are taken at two different intensities above 1 TW/cm^2 (close to the saturation intensity for each atom), and have been scaled to agree at threshold, to illustrate the different energy dependence of the two curves. Both experiment and theory show a large difference between the two atoms in the high energy part of the spectrum, i.e., above 6 eV or approximately 25 MIR photons. Whereas the Na distribution shows essentially no change of slope beyond $3U_p$ (about 3 eV), K exhibits a plateau extending up to the classical limit of $10U_p$. Of particular note is the production of electrons at $10U_p$ corresponding to very strong backscattering. This production of the highest energy
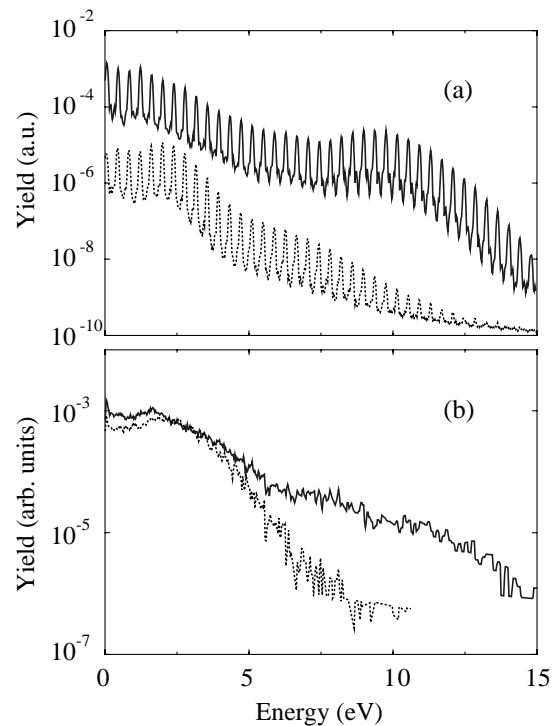

FIG. 1. ATI spectra for potassium (solid line) and sodium atoms (dotted line) excited by 3.2 μm radiation. (a) Theoretical results at 1 TW/cm^2. (b) Experimental spectra at 1.4(5) TW/cm^2 (K) and 1.7(6) TW/cm^2 (Na). The experimental curves have been scaled to agree near threshold.

electrons is much more efficient than that observed in the rare gases [4].

In the wave packet model this strong species dependence is explained by elastic scattering of the returning electron from the different ion cores. Comparison of the K and Na electron-ion pseudopotentials shows that the biggest difference lies in the d channel potential, which is shown as an inset in Fig. 2. We plot the sum of the pseudopotential and the centrifugal term. The hydrogen d potential is included for comparison. The K potential has an attractive well in the d channel, as opposed to Na which is essentially hydrogenic. The s and the p potentials in the two atoms are more repulsive than the analogous hydrogen potentials. For $\ell > 2$ the total potential is dominated by the centrifugal term.

To investigate the role of the d potential in producing high energy electrons, we exchange the K d potential by the H d potential, leaving the s and p potentials unchanged. This modified pseudopotential reproduces the total ionization rate and the low energy portion of the ATI spectrum of the full K atom. In Fig. 2 we show partial ATI rates for K, Na, and the modified K. The Na spectrum has been scaled so that the total yield agrees with the modified K yield. The effect of manipulating the K d potential is remarkable. The high energy part of the spectrum is reduced by almost 2 orders of magnitude when using the H d potential, and is now similar to the Na spectrum. By manipulating one specific feature of the electron-ion potential we can significantly alter the rescattering process.

Our results imply that strong field calculations in the heavier alkali metal atoms using computationally simpler spherically symmetric (ℓ-independent) pseudopotentials will give an incorrect description of the rescattering

process. This is because such a potential, if it is to describe the s and p channels correctly, will always lead to a d potential, which is too repulsive, and consequently to an upward shift of all of the d state energies. We have checked this in K by using the spherical potential of [16], and find that there is no rescattering, in agreement with the results in Fig. 2. We have also tested several nonlocal pseudopotentials which give correct d state energies, and find that the high energy part of the photoelectron spectrum agrees with that shown for K in Fig. 1.

Figure 3 illustrates the rescattering process more quantitatively. We show a measure of the relative efficiency of the scattering process by plotting the ratio of high energy electrons (defined here as electrons with energies above $6U_p$) to the total ionization yield. Results are shown as a function of laser intensity for Na, K, Rb, and the modified K atom, where the d potential has been exchanged by the H d potential. In agreement with Fig. 2, the modified K atom gives results very similar to Na, whereas both K and Rb are efficient rescatterers. This figure demonstrates that the difference in the rescattering efficiency persists at all intensities.

To understand the behavior of the heavier alkali metals, we have also calculated the differential cross section for elastic scattering of an electron wave packet from the ion core potential. The incoming energy of the wave packet is given by the strong field, $3U_p$, and the width is determined by its initial width at tunneling and the spread during the time of propagation in the continuum [5,8]. We have calculated the Coulomb and additional short range phase shifts by numerical integration of the scattering equations for $e^- - K^+$ or $e^- - Na^+$ scattering [5].
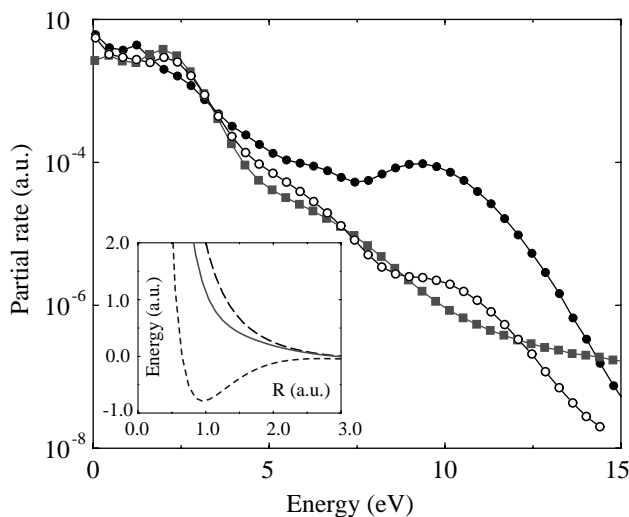

FIG. 2. Partial rates (ionization rate per ATI peak) for K (black circles), Na (squares), and the modified K atom (white circles), where the d potential has been substituted with the H d potential. The intensity is 1 TW/cm². In the inset we show the d potential for K (short-dashed line), Na (solid line), and H (long-dashed line).
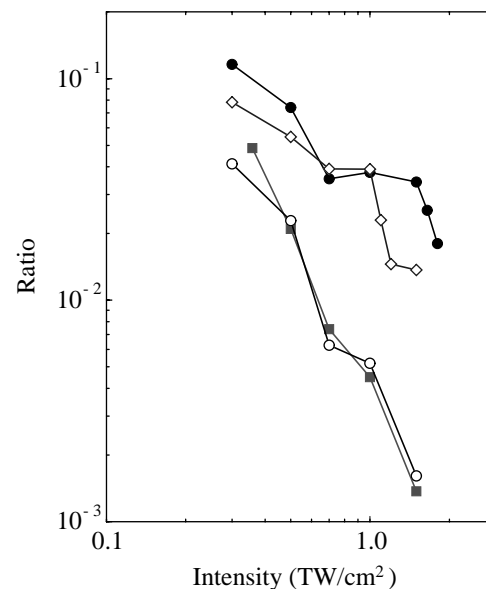

FIG. 3. Calculated ratio of electrons with kinetic energies above $6U_p$ to the total yield is plotted as a function of the intensity, for K (black circles), Na (squares), Rb (diamonds), and the modified K (white circles).
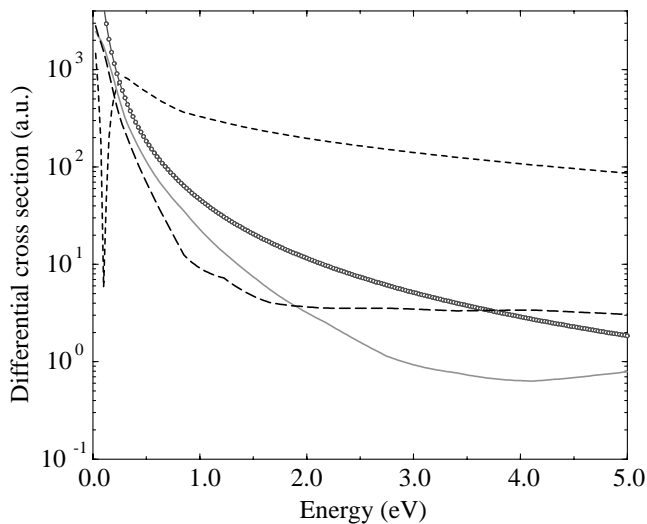
FIG. 4.   Elastic differential backscattering cross sections for K (short-dashed line), Na (solid line), and the modified K (long-dashed line). We show the Rutherford scattering cross section (circles) for comparison.

In Fig. 4 we show the backscattering cross sections ($\theta = \pi$) for K, Na, and the modified K atom. For comparison we also show the H cross section $1/16E^2$, in a.u. We assume a returning wave packet width of 30 a.u. [17]. The K cross section is much larger than that of Na and the modified K, which are both comparable to the Rutherford cross section. Comparing the cross sections at 2.8 eV, which corresponds to the maximum return energy $3U_p$ at an intensity of 1 TW/cm^2, we see that the K cross section is about 50 times larger than the modified K cross section, and 200 times larger than the Na cross section, in good agreement with the relative backscattering efficiencies at about 10 eV shown in Fig. 2. We note that this effect is strongest at large scattering angles. These results show that the difference in the rescattering efficiency originates in the electronic structure of the atoms through the difference in the potential scattering cross section. They also validate the picture of the high energy part of the ATI spectrum as being due to a two-step process, namely elastic scattering off the ion core followed by acceleration in the strong field. However, not all features of above threshold ionization can be explained within this model. The structures observed in the angular distributions, for instance, and the intensity dependent resonances of [6,18] are good examples of this, since they presumedly depend on multiple scattering off the ion core and the resulting interference effects.

We have studied the production of high order photo-electrons in alkali metal atoms in strong MIR laser fields. Since the doubly excited states of the alkali metals have much higher energies than the observed plateau, it is not necessary to invoke correlation effects, such as simultaneous excitation of two electrons, to explain this process. We find a very strong species dependence of the onset and strength of the plateau in the ATI spectra. We have demon-

strated that this difference originates in specific features of the potential experienced by the valence electron in the presence of the ion core. By modifying the potential in a single partial wave we can change the elastic scattering cross section, and therefore the rescattering efficiency, by 2 orders of magnitude. That two potentials leading to the same initial ionization dynamics can give rise to vastly different high energy photoelectron distributions reflects the fact that the atomic structure is never negligible since the scattering takes place at short range.

[1] B. Sheehy and L. F. DiMauro, Ann. Rev. Phys. Chem. **47**, 463 (1996).
[2] K. J. Schafer et al., Phys. Rev. Lett. **70**, 1599 (1993).
[3] P. B. Corkum, Phys. Rev. Lett. **71**, 1994 (1993).
[4] G. G. Paulus et al., Phys. Rev. Lett. **72**, 2851 (1994).
[5] B. Walker et al., Phys. Rev. Lett. **77**, 5031 (1996).
[6] B. Yang et al., Phys. Rev. Lett. **71**, 3770 (1993).
[7] U_p measured in eV is given by $0.093I\lambda^2$, where I is the intensity in TW/cm^2 and λ is the wavelength in microns. The long wavelength, high intensity limit is defined by U_p being substantially larger than the photon energy. For 1 TW/cm^2, 3.2 μm light U_p is 1 eV, which corresponds to about 3 MIR photons.
[8] W. Becker et al., J. Phys. B **27**, L325 (1994).
[9] G. G. Paulus et al., J. Phys. B **27**, L703 (1994).
[10] M. Lewenstein et al., Phys. Rev. A **51**, 1495 (1995).
[11] B. Sheehy et al., in *Proceedings of the Eighth International Conference on Multiphoton Processes,* edited by R. R. Freeman, K. C. Kulander, and L. F. DiMauro (AIP, New York, 2000).
[12] G. G. Paulus et al., J. Phys. B **29**, L249 (1996).
[13] K. C. Kulander, K. J. Schafer, and J. L. Krause, in *Atoms in Intense Laser Fields,* edited by M. Gavrila (Academic Press, New York, 1992).
[14] W. J. Stevens et al., Can. J. Chem. **70**, 612 (1992).
[15] E. Cormier and P. Lambropoulos, J. Phys. B **29**, 1667 (1996); H. G. Muller, Laser Phys. **9**, 138 (1999).
[16] J. N. Bardsley, in *Case Studies in Atomic Physics* (North-Holland, Amsterdam, 1974), Vol. 4, p. 302.
[17] For widths larger than about 10 a.u., the results are essentially independent of the width, for energies above 0.5 eV.
[18] M. P. Hertlein et al., J. Phys. B **30**, L197 (1997); M. J. Nandor et al., Phys. Rev. A **60**, R1771 (1999).